Zhao, Weixin; Kilpeläinen, Simo; Kosonen, Risto; Jokisalo, Juha; Lestinen, Sami; Mustakallio, Panu

Thermal environment and ventilation efficiency in a simulated office room with personalized micro-environment and fully mixed ventilation systems

Published in:
Building and Environment

DOI:
10.1016/j.buildenv.2020.107445

Published: 15/01/2021

Document Version
Peer-reviewed accepted author manuscript, also known as Final accepted manuscript or Post-print

Please cite the original version:
Zhao, W., Kilpeläinen, S., Kosonen, R., Jokisalo, J., Lestinen, S., & Mustakallio, P. (2021). Thermal environment and ventilation efficiency in a simulated office room with personalized micro-environment and fully mixed ventilation systems. *Building and Environment*, *188*, Article 107445.
https://doi.org/10.1016/j.buildenv.2020.107445

Journal Pre-proof

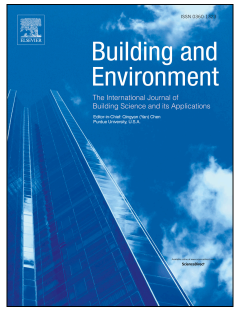

Thermal environment and ventilation efficiency in a simulated office room with personalized micro-environment and fully mixed ventilation systems

Weixin Zhao, Simo Kilpeläinen, Risto Kosonen, Juha Jokisalo, Sami Lestinen, Panu Mustakallio

PII: S0360-1323(20)30812-X

DOI: https://doi.org/10.1016/j.buildenv.2020.107445

Reference: BAE 107445

To appear in: *Building and Environment*

Received Date: 29 June 2020

Revised Date: 16 October 2020

Accepted Date: 3 November 2020

Please cite this article as: Zhao W, Kilpeläinen S, Kosonen R, Jokisalo J, Lestinen S, Mustakallio P, Thermal environment and ventilation efficiency in a simulated office room with personalized micro-environment and fully mixed ventilation systems, *Building and Environment* (2020), doi: https://doi.org/10.1016/j.buildenv.2020.107445.

Thermal environment and ventilation efficiency in a simulated office room with personalized micro-environment and fully mixed ventilation systems

Weixin Zhao [a, *], Simo Kilpeläinen [a], Risto Kosonen [a, b] Juha Jokisalo[a], Sami Lestinen [a], Panu Mustakallio [c]

[a] Aalto University, Department of Mechanical Engineering, Finland

[b] College of Urban Construction, Nanjing Tech University, China

[c] Halton Oy, Finland

[*]Corresponding author: weixin.zhao@aalto.fi

Abstract

One of the major challenges in modern buildings is to guarantee healthy indoor air quality and excellent thermal comfort in an energy efficient manner. In this study, the performance of a micro-environment system combined radiant panel and convective flow was designed and compared to an all-air diffuse ceiling ventilation (DCV) system. In the analyzed micro-environment system of personalized ventilation and radiant panel (PVRP), two local personal air terminal devices supplied clean air directly to occupants. The radiant panels were used to satisfy the required cooling load. The results show that the air change efficiency with the PVRP was over 60% which was better than the fully mixing flow (50%). The mean age of air of personalized airflow system was smaller at the micro-environment near the workstation than the DCV despite the airflow rate was much lower. Furthermore, the air temperature near the workstation can be maintained at designed value with the PVRP and the draught rate can be kept at acceptable level. Furthermore, the vertical temperature difference did not cause thermal discomfort with the PVRP system near the workstation.

Keywords: Personalized ventilation, Micro-environment system, Radiant panel cooling, Diffuse ceiling all-air system, Thermal comfort, Ventilation efficiency

1. Introduction

In modern cities and urban societies, the office workers spend majority of their time inside a building. People look forward to work at a satisfactory indoor climate which could provide superior thermal comfort and indoor air quality [1,2]. Acceptable and comfortable indoor environment within air-conditioned and ventilated indoor spaces, especially office rooms, will lead to an increase in workers' concentration and productivity. As a result, there are demands to design novel systems to create higher indoor climate and less energy consumption at the same time [3,4].

There are already some guidelines [5–7] to regulate the ventilation rate (4-10 l/s/person of fresh air) into office rooms. However, actual volume of inhaled air is only 0.1 l/s/person [8]. Hence, the air really inhaled by occupants just accounts minor part of the supplied volume.

It has been proved that the diffuse ceiling ventilation (DCV) system can provide a better indoor environment because of low-impulse supply from the large ceiling area [9,10]. However, with the DCV, thermal plumes dominate the air distribution in the room space and supply air from the perforated ceiling is the minor factor in mixing [11].

In normal enclosures, occupied zone required control of indoor climate conditions make up just a small volume of the whole space [12]. Therefore, a uniform indoor environment needs to be converted to a non-uniform one accommodated by personal preferences [13]. Also, the target area should be controlled only during occupants' presence. The occupancy-based system can promote thermal comfort in warm environments [14,15]. By this way, energy is used only where it is really required to meet the individual indoor air perception and thermal comfort [16,17]. The previous study showed the considerable energy saving (up to 75%)can be achieved by adapted individually controlled indoor environmental devices [18].

There are some designs for individually controlled micro-environment in the office [19,20] e.g. a heating chair and a desk-mounted air terminal device of personalized ventilation [21]. Shao et al. [22] developed the multi-mode ventilation strategy with several single airflow patterns by utilizing the individual merits of single airflow pattern. The ventilation strategy met variable demand scenarios according to variations of distribution of occupants and heat load. Similarly, the non-uniformity of air distribution was used to control thermal conditions of the subzones to maximally satisfy the thermal preference [23]. Personal comfort systems (PCS) included a heated shoe insole, heated/cooled wristpad, small deskfan, and heated/cooled chair to provide high heating and cooling coe□cient and high whole-body thermal acceptance and thermal comfort perception [24].

Personalized ventilation (PV) has potential to improve the perceived air quality by supplying clean and cold air directly to occupants, i.e. where and when it is required [25]. The personalized airflow increases the personal thermal comfort because of the convective cooling effect [26]. The users can control the direction, airflow rate and temperature of personalized supply air to accommodate the individual preferences. Several researches have shown that PV combined with traditional mechanical ventilation systems increase perceived air quality [27,28] and personal thermal comfort [29,30].

Supplying cooling load only by convective effect of high airflow rate might cause thermal discomfort [31,32]. In order to minimize the draught rate in the occupied zone, an air-water system can be induced. For example, radiant cooling panels can be used to supply cooling load by water. By using radiant cooling systems and less airflow rate, air movement at the occupied zone could be reduced [33,34].

In the earlier study, the low velocity unit combined with the radiant panel (LVRP) was introduced [35]. In that concept, the air was supplied downward over the head from 2.1 m level. Presently, there are no studies of a system where the micro-environment around the workstation is cooled with the personalized ventilation and radiant cooling panels (PVRP) supported with the diffuse ceiling all-air system for background ventilation. In the present concept (PVRP), the local airflow is distributed to dummy horizontally. The main goal of this paper is to design and analyze the performance of a personal air terminal unit combined with the radiant panel (PVRP) system over the occupant in the office. The distribution of room air temperature and velocity in the micro-environment close to the workstation, as well as their effect on the ventilation efficiency and local thermal comfort, were analyzed. The different parameters of indoor environment were compared between the PVRP system and the reference system - diffuse ceiling ventilation (DCV) [36] under the same conditions.

Section 2 introduces the test chamber and experimental methods to analyze the PVRP system. Section 3 compares the performance of the PVRP and DCV systems regarding the airflow pattern, ventilation effectiveness and thermal comfort. Section 4 discusses the merits of the PVRP system and raises the further studies. Section 5 concludes the performance of the PVRP system based on the results.

Nomenclature			
$T_{\mathrm{ave}(0.1-1.1)}$	mean air temperature from the height of 0.1 m to 1.1 m [°C]	PVRP	personalized ventilation and radiant panel system
T_{ex}	mean exhaust air temperature [°C]	DCV	diffuse ceiling ventilation
$t_{a,l}$	local air temperature [°C]	HRE	heat removal efficiency

T_{su}	mean supply air temperature [°C]	WS	workstation
SD	standard deviation of the velocity [m/s]	ATD	air terminal device
$\bar{u}$	mean air speed [m/s]	MAA	mean age of air [minute]
u_{SD}	standard deviation of fluctuating velocity (m/s)	τ_n	nominal age of air [minute]
DR	draught risk [%]	LAC	local air change index [%]
Tu	local turbulence intensity [%]	$\overline{\tau_P}$	local mean age of air [minute]
$\bar{u}_{a,l}$	local mean air speed [m/s]	ACE	air change efficiency [%]
$\overline{\tau_r}$	actual air change time [minute]	$\langle\tau\rangle$	mean age of air [minute]

2. Methods

The test chamber layout is introduced firstly with designed heat gains. Then the analyzed personalized ventilation combined with the radiant panel (PVRP) system and the reference system of all-air diffuse ceiling ventilation (DCV) are presented. The designed parameters of the analyzed systems are introduced. After that, we show how the physical measurements are conducted. Finally, experimental errors and uncertainty are analyzed in this section.

2.1. Set-up of test chamber and analyzed systems

A mock-up of a prototypical office with two identical workstations (WS) (Fig. 1) was located in a test chamber with dimension of 5.5 (length) × 3.8 (width) × 3.2 (height) m and the floor area was 20.9 m^2. There was a desk with an air terminal device (ATD) for personalized ventilation (PV) at each workstation. The test chamber was located inside a laboratory hall, ensuring a stable environment outside the chamber. In Nordic conditions, new office buildings are designed to be very airtight. Thus, infiltration was not considered in this study. The pressure difference over the envelope in the test room was monitored and adjusted to be slightly over pressure (1 Pa).

To evaluate the property of the PVRP, it was compared with the all-air system- diffuse ceiling ventilation (DCV) studied earlier in the same set-up condition. The designed heat gains include 60 W/floor-m^2 (usual heat gain level) and 80 W/floor-m^2 (peak heat gain level) in the chamber. Peak heat load was formed by introducing a higher surface temperature of the window panel and computer central unit in addition to the other heat gains i.e. occupants, heated foil on floor, laptop, monitor and lighting. Fig. 1 a) shows the set-up of the test chamber with the PV terminal device and radiant panels system (PVRP). Fig. 1 b) presents the set-up of the reference all-air diffuse ceiling (DCV) system [36], which is a dedicated outdoor air system.

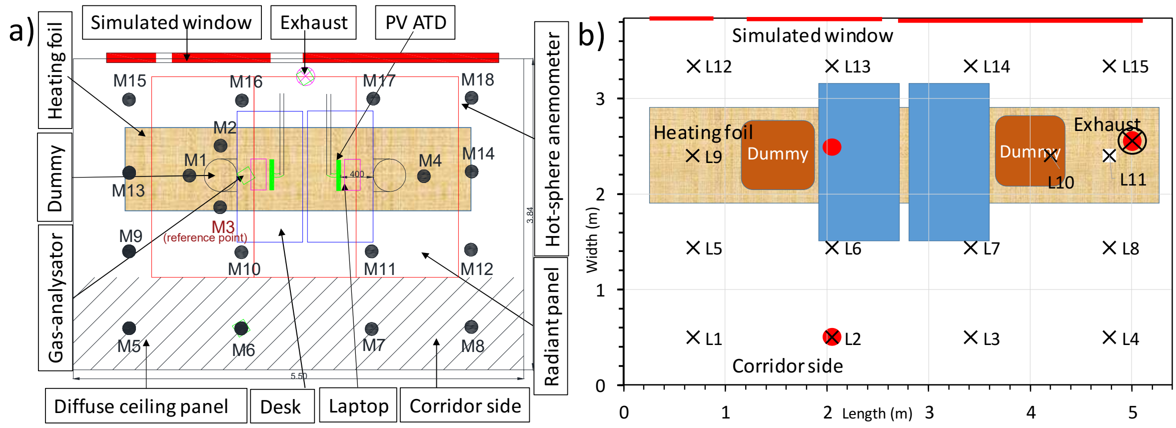

Fig. 1. Test chamber set-up of a) the local personal air terminal devices with the radiant panel system (PVRP) and DCV as background ventilation at corridor side and b) the diffuse ceiling all-air ventilation system (DCV) alone. M1-M18 describes the measured locations by hot-sphere anemometer with the PVRP system; L1-L15 describes the measured locations by hot-sphere anemometer with the DCV system, respectively.

Fig. 2 shows the layout of two systems (PVRP and DCV) included in both workstations (WS). There were a dummy [37] and laptop at each WS. In this physical measurement, the dummies were used as the heat gain of the occupants in the office. In this study, the heat gain was selected to correspond to an activity level of 1.6 met (light activity). This value describes activity level in real office work according the findings of Mishra [38] and Zhai et al. [39]. That value is higher than normally used 1.0-1.2 met activity level of sedentary work. Lights were installed over the workstations. The specific heat gain of light was 5.8 W/m^2, which is typical value for the modern office. The simulated warm window surface was mimicked by with the heated panels where heated water circulates. The surface temperature of the panels was varied between 31-36°C in the 60 W/m^2 case to simulate a sunny day and 33-40°C in the 80 W/m^2 case to simulate the peak solar heat gain [40,41]. The floor was covered by an electric heating foil (5.0 m×1.0 m) to represent direct solar radiation on the perimeter zone (see Fig. 1). The floor surface temperature on the heating foil perimeter area was 33.6°C. In the tests, the heating power of the foil was constant. The surface temperature of unheated floor and walls was 21.7-22.0°C.

There were two computers at each workstation, one laptop and one computer with central unit under the desk and a separate monitor. The central unit was simulated with an additional heat source of 0.4 × 0.4 × 0.4 m^3 locating on the floor below the desk.

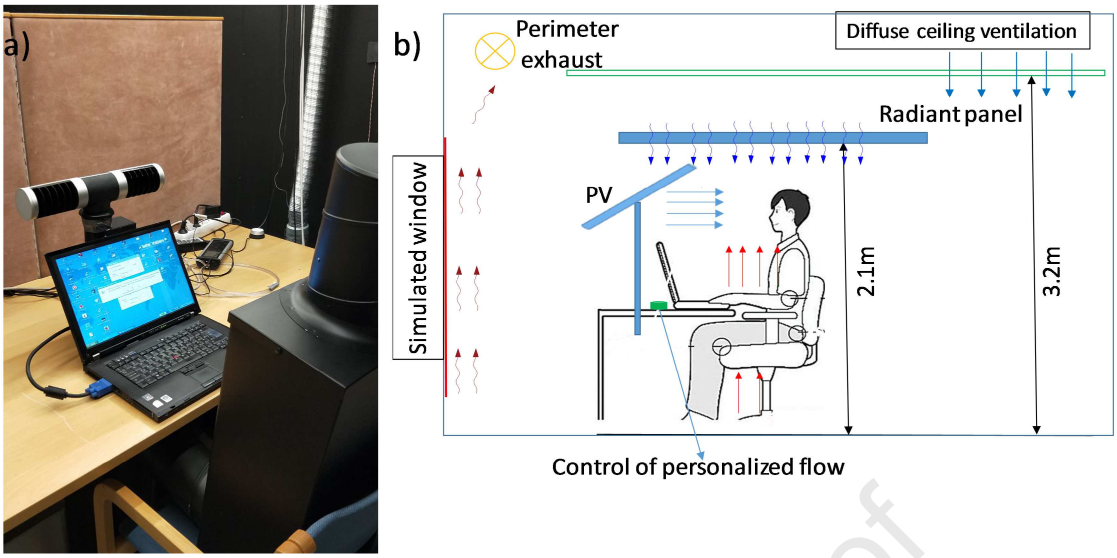

Fig. 2. a) The set-up of WS with the seated dummy and PV ATD and b) a draft of PVRP system and perimeter exhaust.

Table 1

All the heat gains used in the measurements.

Heat flux	Dummies (2 pc.)	Laptops (2 pc.)	Monitors (2 pc.)	Window panels (7 pc.)	Light	Computer model at floor	Solar heat gain at floor	Total heat gain
($W/floor-m^2$)	(W)	(W)	(W)	(W)	(W)	(W)	(W)	(W)
80	188	75	78	693	116	103	420	1676
60	188	75	78	381	116	0	420	1258

Two PV ATDs were installed on the desk at 40 cm distance from the dummy to supply fresh and cold air directly to the breathing zone. The designed supply airflow rates were 7 l/s, 10 l/s or 15 l/s from each PV ATD. The airflow rates 10 l/s and 7 l/s given per person were according to Standard EN15251 [5] Category A and B for a non-residential building. The airflow rate 15 l/s given per person was according to EN13779 [42] Category IDA 1 where the occupants are only sources of pollution.

Above the two workstations, three perforated radiant cooling panels (2400 mm x 1200 mm) were installed to provide local cooling load (Fig.3). The radiant panels were installed at 2.1 m height so that even a tall person could easily walk under the panel. The connection of water pipes Ø = 12 mm is presented in Fig. 3a). The radiant panels were uninsulated, leaving the panel area open for free convection through the panels. The average surface temperature of the radiant panels was 20°C.

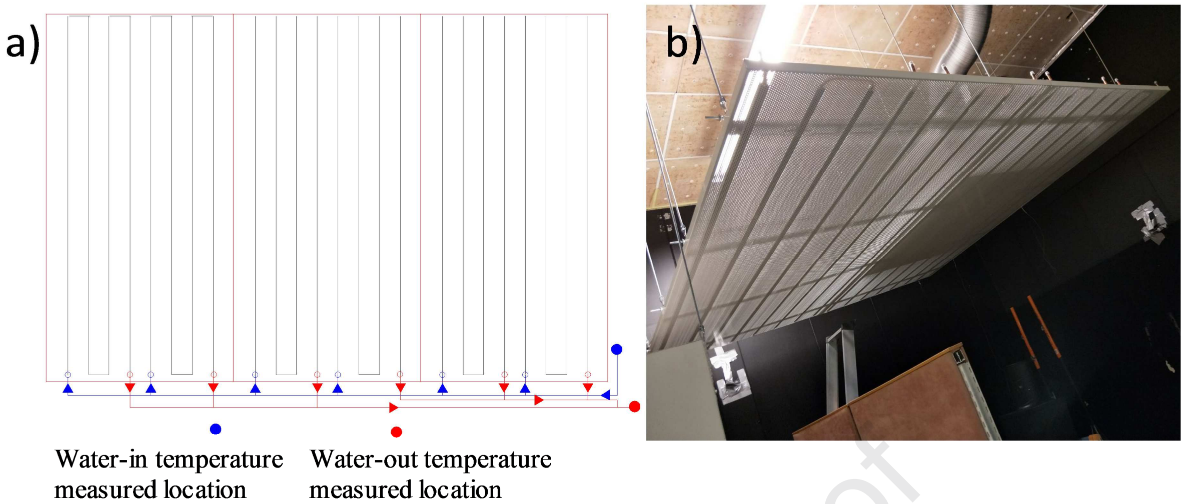

Figure 3. a) The connection of water pipes with three radiant cooling panels and b) installation of radiant cooling panels above two workstations.

At the corridor side, the DCV was used as background ventilation to supply some airflow with the PVRP system. The measurement location M3 was selected as a reference temperature location at the height of 1.1 m. The selected location (M3) close to the workstation can represent temperature at the occupied zone. The height of 1.1 m represents thermal comfort of a sitting person. At the simulated window side, there was an exhaust grille to directly capture a major part of the convective flow from the heated window (see Fig. 2b).

Contrary to the PVRP where only a part of the DCV panels were used, the outdoor air was supplied from the whole ceiling area with the DCV concept alone. The exhaust temperature was used as a reference temperature with the DCV (Fig. 1b). The reference temperature was maintained at 26.0°C with the PVRP and DCV systems.

2.2. Experimental facilities and instruments

There were total 18 measured points (M1-M18) with the PVRP and 15 measured points (L1-L15) with the DCV systems in the chamber (Fig. 1) to evaluate the thermal environment. In this study, three measurement points (M1-M3) located at the both sides of the dummy and behind the dummy were used to evaluate average thermal conditions close to the workstation with the PVRP. The location in front of the dummy was not used because that location may have influence on the direct airflow from the PV unit. Thus, it describes the effect of air throwing properties of the PV. The parameters including air temperature, air velocity, turbulence intensity and draught risk were measured with hot-sphere anemometers (with accuracy of ±0.02 m/s ± 2% reference velocity and ± 0.2°C on reference temperature, 2Hz) at the height of 0.1 m, 0.6 m, 1.1 m and 1.7 m at each measured point. The operative temperature (with accuracy of ± 0.3°C) was measured at 1.1 m height [43] at M3 (reference location) with the PVRP by Dantec (see Fig. 1a). The mean radiant temperature was calculated by the same device.

All the measurement equipment was calibrated before the measurements were conducted. Before the measurements, the marker smoke was released from the air inlet duct to visualize the indoor airflow pattern. High intensity lights and a video camera were used to record the airflow patterns. Each test was conducted under stable conditions and each location was measured 10 minutes [44].

In this study, ventilation efficiency was evaluated by measuring concentration of tracer gas CO_2 and analyzed by the tracer-down method [45]. The reason was that the size of CO_2 molecules is similar to the other molecules in the air. CO_2 concentration was measured with the PVRP at two points at the height of 1.1 m (one located near the dummy and another at an unoccupied zone– M6) and one location at the exhaust (EX) to evaluate the air change efficiency (ACE) in the whole space. With the DCV, CO_2 concentration was measured at three points (red point in Figure 1 b): one at the dummy, one at the exhaust and one at the unoccupied zone.

Due to the heating and cooling load balance, the total airflow rates used with the two heat gains were different with the DCV system alone, as shown in Table 2. With the PVRP system, the supplied total airflow rate (from the PV and DCV) was kept the same (42 l/s) with 60 W/floor-m² and 80 W/floor-m² (Table 3). Thus, the airflow rate with the air-water system (PVRP) was much lower than with the all-air system (DCV). The temperature of air supplied from the PV ATD device was maintained at 20°C. Supply air temperature from the DCV was 15°C. Table 4 shows the water flow rate circulated in the radiant panel pipes based on the cooling load required in the chamber.

Table 2

The airflow parameters at the two heat gain levels with the DCV system.

Heat flux (W/floor-m²)	Room air temperature (°C)	Required airflow rate (l/s)	Supply air temperature (°C)
80	26	153	17
60	26	118	17

Table 3

The airflow rates and parameters of the PV ATD and background ventilation with the PVRP system.

Airflow rate of each PV terminal	Airflow rate at unoccupied zone (DCV)	Total airflow rate	Supply air temperature of PV	Supply air temperature of DCV (background)
(l/s)	(l/s)	(l/s)	(°C)	(°C)
7	28	42	20.0	15.0
10	22	42	20.0	15.0
15	12	42	20.0	15.0

Table 4

Cooling load balance between the supplied air and cooling water with the PVRP under different designed heat gains.

Total heat flux	Total heat gain	Supply air cooling capacity	Inlet water temperature	Outlet water temperature	Water flow rate	Radiant panel cooling capacity
(W/floor-m²)	(W)	(W)	(°C)	(°C)	(kg/s)	(W)
80	1680	600	15	16.9	0.10	1080
60	1260	590	15	16.5	0.09	670

2.3 Experimental errors and uncertainty

Experimental error is the difference between the measured value and the true value or between two measured values. Experimental error is evaluated by its accuracy and precision. Accuracy measures how close a measured value is to the true value or accepted value. Since a true or accepted value for a physical quantity may be unknown, it is sometimes not possible to determine the accuracy of a measurement. Precision measures how closely two or more measurements agree with other. Melikov et al. [46] proposed that the minimum realistic absolute expanded uncertainty at the 95% confidence is $dU = \pm(0.025 + 0.025U)$ for the mean air velocity. This means that the typical mean air velocity levels are correspondingly e.g. 0.1 ± 0.028 m/s and ± 28% and 0.2 ± 0.03 m/s and ± 15%, respectively. Consequently, the relative uncertainty increases towards lower air velocity levels and dominates the uncertainty of functions on airflow characteristics. The uncertainty of hot-sphere anemometers is ±0.02 m/s ± 2% reference velocity, therefore, the typical mean air velocity levels are correspondingly e.g. 0.1 ± 0.022 m/s and ± 22% and 0.2 ± 0.024 m/s and ± 12%, which uncertainty is lower.

2.4 Evaluation indices

Performance of the PVRP system regarding to thermal comfort and ventilation efficiency for the di□erentiated zonal environment was analyzed.

The distribution of air temperature and velocity were measured at heights of 0.1 m, 0.6 m, 1.1 m and 1.7 m, which represent the ankle level, the waist level, the head level and the boundary of the occupied zone in the whole space, respectively.

The local thermal discomfort was evaluated by the draught risk index. Draught represents the unwanted local cooling of a human body caused by air movements. The DR is as given by Eq. (1)

$$DR = \left(34 - t_{a,l}\right)\left(\bar{u}_{a,l} - 0.05\right)^{0.62}\left(0.37 \cdot \bar{u}_{a,l} \cdot Tu + 3.14\right) \quad (1)$$

where $t_{a,l}$ is the local mean air temperature, $\bar{u}_{a,l}$ is the local mean air speed from 0.05 m/s to 0.5 m/s, and Tu is the local turbulence intensity in percent from 10% to 60% . If $\bar{u}_{a,l}$ <0.05, use $\bar{u}_{a,l}$=0.05; if DR> 100%, use DR=100%. According to ISO 7730 standard [47], DR<10% meets the Category A of thermal environment; DR<20% meets the Category B. Category A means the high level of expectation to indoor environment and is recommended for spaces occupied by very sensitive and fragile persons with special requirements while Category B means the normal level of expectation.

Turbulence intensity (Tu) is defined by Eq. (2), as

$$Tu = \frac{u_{\mathrm{SD}}}{\bar{u}} \times 100 \quad (2)$$

where u_{SD} means the standard deviation of fluctuating velocity and $\bar{u}$ means the mean air velocity.

Heat removal efficiency (HRE) [48] is proposed to measure the effectiveness of heat removal from a space as Eq. (3)

$$\mathrm{HRE} = \frac{T_{ex} - \mathrm{T}_{su}}{T_{\mathrm{ave}(0.1-1.1)} - \mathrm{T}_{su}} \quad (3)$$

where $T_{\mathrm{ave}(0.1-1.1)}$ means the mean air temperature from the height of 0.1 m to 1.1 m, $\bar{T}_{ex}$ means the temperature at exhaust terminal and T_{su} means the supply air temperature.

The heat removal efficiency is used to evaluate the capability of ventilation and cooling systems to create a local micro-environment close to the workstation. In practice, that means temperature difference between the occupied zone and exhaust.

Ventilation efficiency of the PVRP and DCV system was analyzed by the concept of the air change efficiency (ACE), which is used to evaluate how fast the air can be replaced in a room compared to the theoretically fastest rate with the same ventilation airflow [45].

The actual air change time $\overline{\tau_r}$ can be derived from the room mean age of air (MAA) $\langle\overline{\tau}\rangle$ and it is defined as Eq. (4).

$$\overline{\tau_r} = 2\langle\overline{\tau}\rangle \tag{4}$$

Air change efficiency (ACE) can be explained as the ratio between the theoretically shortest possible air change time (nominal age of air) τ_n [49] to of the average time it takes to replace the air in the room $\overline{\tau_r}$ as Eq. (5)

$$\epsilon^a = \frac{\tau_n}{\overline{\tau_r}} \cdot 100\% \tag{5}$$

where ϵ^a is the air change efficiency (ACE), $\langle\overline{\tau}\rangle$ is the mean age of air (MAA) *and* $\overline{\tau_r}$ is the actual air replacement time.

Because ACE is also the ratio between τ_n and τ_r, the Eq. (5) can be shown as:

$$\epsilon^a = \frac{\tau_n}{2\langle\overline{\tau}\rangle} \cdot 100\% \tag{6}$$

The local air change index (LAC), ϵ_P^a, specifies the ventilation efficiency of local condition, as the ratio between the nominal age of air (τ_n) to the local mean age of air ($\overline{\tau_P}$), in Eq. (7)

$$\epsilon_P^a = \frac{\tau_n}{\overline{\tau_P}} \cdot 100\% \tag{7}$$

The local air change index was calculated at the CO_2 measurement points included near the dummy and M6 with the PVRP system.

The mean age of the room air is calculated from the weighted area under the curve using Equation (8) [49]

$$\langle\bar{\tau}\rangle = \frac{\sum_{i=1}^{i=n}\left[\frac{c_i + c_{i-1}}{2}\cdot(t_i + t_{i-1})\cdot\frac{t_i + t_{i-1}}{2}\right] + \frac{c_n}{\theta}\cdot\left[\frac{1}{\theta} + t_n\right]}{\sum_{i=1}^{i=n}\left[\frac{c_i + c_{i-1}}{2}\cdot(t_i - t_{i-1})\right] + \frac{c_n}{\theta}} \tag{8}$$

The nominal time constant is calculated by Equation (9):

$$\tau_n = \frac{\sum_{i=1}^{i=n}\left[\frac{c_i + c_{i-1}}{2}\cdot(t_i - t_{i-1})\right] + \frac{c_n}{\theta}}{c_0} \tag{9}$$

where c_i is the concentration of CO_2 at time $t = i$, $and\ \theta$ is the absolute value of the slope of the decay curve.

3. Results

Based on the experiments conducted in the test chamber, the airflow pattern of the PVRP was shown by using the smoke. The heat removal efficiency was compared between the perimeter exhaust and the standard exhaust valve. Then the indoor air quality regarding with age of air and air change efficiency was analyzed. At last, the thermal comfort including temperature profile, velocity profile and draught risk were shown.

3.1. Airflow visualization of smoke test

The airflow structure of the PV around the workstation was visualized by the maker smoke to assess the airflow pattern of the PVRP system. When the personalized airflow rate was at the minimum setting (7 l/s), the air jet turned slightly upward because of the combined buoyancy flow of the computers and dummy (Fig. 4 a). However, the jet still reached the breathing zone. The momentum flux of the jet overcame the effect of the buoyancy effect, and the jet was able to approach the dummy when the personalized airflow rate was increased to 15 l/s. The central axis of the jet was aligned with the level of the subject's chest and after the jet collided with the dummy, it turned both downwards and upwards along the body. Hence, the personalized airflow entrained the convective boundary layer existing the human body and cooled down the upper body. It should be noted that the smoke visualization presented the performance without breathing effect. In the case of a real person, especially when using low supply airflow rate, the effects of inhalation and exhalation can reduce the ventilation efficiency, which is not considered in this study.

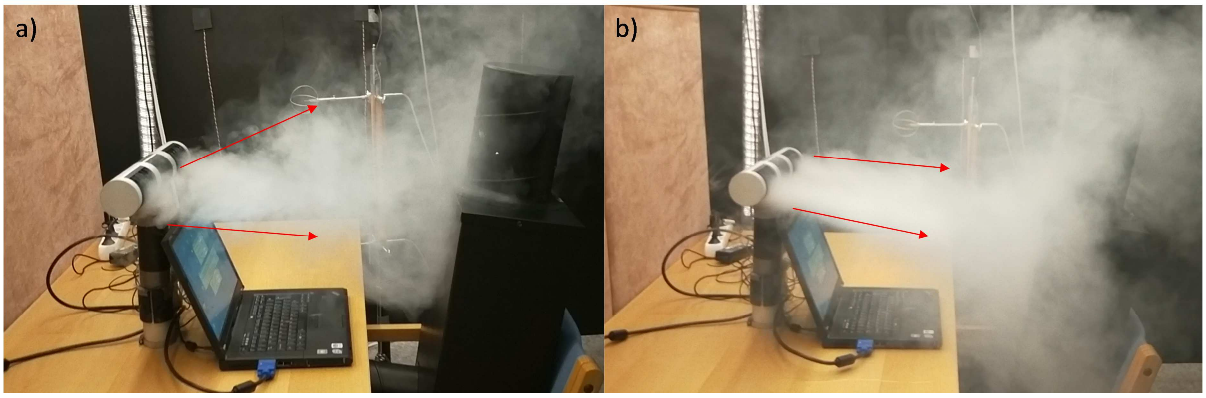

Fig. 4. Smoke visualization of the personalized airflow pattern with a) 7 l/s and b) 15 l/s. The red arrows mean the main direction of the air jet.

3.2. Heat removal efficiency

Table 5 shows the heat removal efficiencies of the all-air DCV were 0.96 and 1.02 with the standard exhaust valve and the heat gains of 60 W/floor-m^2 (118 l/s) and 80 W/floor-m^2 (153 l/s), respectively. With the all-air system, a small temperature difference exits which also affects the HRE because of heat gain distribution and the number of airflow rates. With the perimeter exhaust and PVRP system, the HRE was increased from 1.03 to 1.07 when the personalized airflow rate was increased from 7 l/s to 15 l/s with 60 W/floor-m^2. The corresponding values were 1.03 (7 l/s) and 1.11 (15 l/s) with 80 W/floor-m^2 (Table 5). It should be noted that the total supplied airflow rate was constant at 42 l/s for the both studied heat gain levels in the PVRP case. As a result, the HRE was improved with the increasing heat gain and personalized airflow rate, with the personalized airflow rate being stronger of the two. As shown in Table 5, the HRE was better with the PVRP already at 7 l/s than with the DCV system. One reason for this was that the perimeter exhaust could capture the majority of the convective thermal plume of the simulated window and radiation heat gain from the window entered mostly to the whole space. Another reason was that the personalized airflow solution can provide spot cooling at the workstation. Therefore, the air temperature in the micro-environment at the workstation was lower with the PVRP than with the fully mixed system (DCV).

Table 5

Heat removal efficiency of the PVRP and DCV systems.

HRE	60 W/floor-m^2	80 W/floor-m^2
DCV	0.96	1.02
PVRP (7/28 l/s) [a]	1.03	1.03

PVRP (10/22 l/s) [b]	1.06	1.04
PVRP (15/12 l/s) [c]	1.07	1.11

[a] The airflow rate from each PV ATD was 7 l/s and the rest of airflow rate was 28 l/s from the DCV, the total airflow rate was 7*2+28=42 l/s

[b] The airflow rate from each PV ATD was 10 l/s and the rest of airflow rate was 22 l/s from the DCV, the total airflow rate was 10*2+22=42 l/s

[c] The airflow rate from each PV ATD was 15 l/s and the rest of airflow rate was 12 l/s from the DCV, the total airflow rate was 15*2+12=42 l/s

3.3. Ventilation efficiency

3.3.1. Mean age of air

Fig. 5 shows the distribution of the mean age of air (MAA) near the dummy and in the unoccupied zone with the PVRP and DCV systems. With the case of 60 W/floor-m^2 and personalized airflow rate of 7 l/s, the MAA was 25.4 minutes near the dummy with the PVRP. It was nearly the same in the unoccupied zone at M6 (25.5 minutes). The reason was that less personalized airflow and more background airflow of DCV created a rather uniform environment in the whole space. If the personalized airflow rate was 15 l/s, MAA was 22.6 minutes near the dummy and 26.7 minutes in the unoccupied zone, respectively. This indicates that personalized ventilation had a noticeable effect on the MAA near the dummy at higher airflow rates. As the total flow rate (42 l/s) of the PVRP was kept the same all the time, MAA decreased near the dummy and increased in the unoccupied zone, respectively.

With the PVRP, MAA near the dummy was smaller with heat gains of 80 W/floor-m^2 than 60 W/floor-m^2 at different personalized airflow rates. With 80 W/floor-m^2, the higher heat gain of the computer central unit, warmer window surface and higher radiant cooling of the panel accelerated the air replacement in the room compared with the case of 60 W/floor-m^2. As a result, the higher heat gain level enhanced the performance of ventilation close to the workstation and contributed to the decline of the mean age of air. It should be noted that the interaction of several flows was rather complex when the thermal load is higher.

With the DCV system, the average MAA was 25.2 minutes near the dummy and at a slightly higher level (26.4 minutes) in the unoccupied zone (L2) under 60 W/floor-m^2. Therefore, MAA was smaller near the dummy and higher in the unoccupied zone (M6) with the PVRP compared to the DCV system. Even though the total airflow rate of the DCV system was 2.8 times higher than with the PVRP, MAA was lower. The reason was that the supply air was quite evenly distributed to the whole space with the DCV while the PVRP supplied part of the air directly to the occupied zone. Thus, the ventilation efficiency was higher with the local supply arrangement.

With the DCV, MAA was shorter with 80 W/floor-m^2 (22.2 minutes) than with 60 W/floor-m^2 (25.2 minutes). This is because the supplied airflow rate of DCV was increased significantly by 30% from 118 l/s to 153 l/s which accelerated the air replacement and then decreased the MAA with the increasing heat gain from 60 W/floor-m^2 to 80 W/floor-m^2 in the ventilated space.

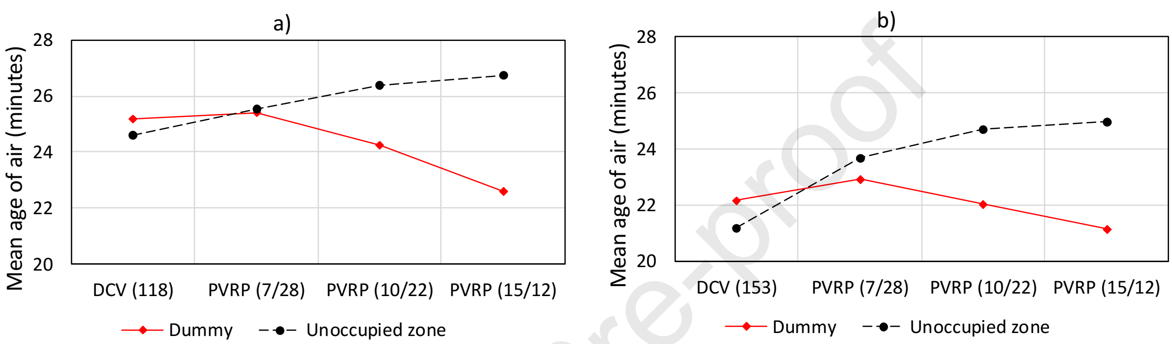

Fig. 5. The distribution of MAA air under the DCV and PVRP systems with a) 60 W/floor-m^2 and b) 80 W/floor-m^2.

3.3.2. Local air change index

Fig. 6 shows that the distribution of local air change index (LAC) was inverse to the distribution of MAA. LAC of the PVRP system was around 130% near the dummy with all the three personalized airflow rates under 80 W/floor-m^2. However, for the DCV the index was 101%, corresponding to fully mixed conditions. Therefore, the PVRP replaced air faster in the micro-environment close to the workstation compared to the DCV. In addition, LAC increased from 129% to 133% near the dummy and reduced in the unoccupied zone (M6) with the increasing personalized airflow rate from 7 l/s to 15 l/s. Therefore, with increasing the personalized airflow rate from 7 l/s to 15 l/s with the PVRP system, local indoor air quality may slightly be enhanced in the micro-environment.

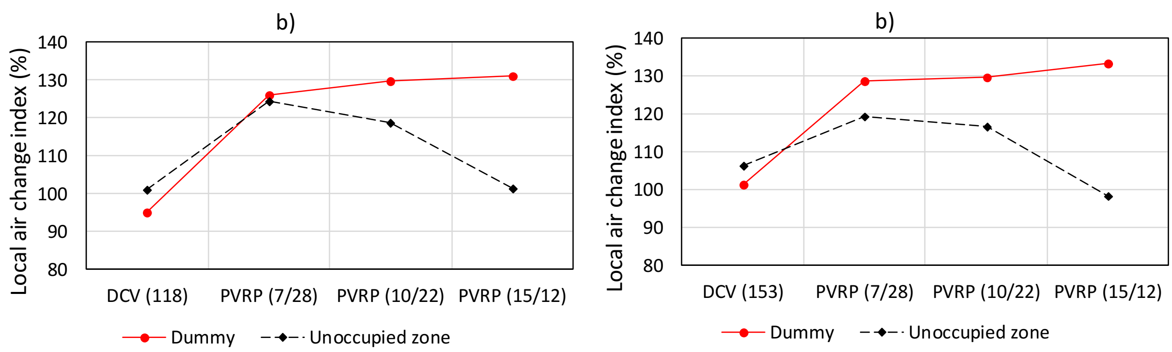

Fig. 6. The distribution of LAC indices with the DCV and PVRP systems under a) 60 W/floor-m^2 and b) 80 W/floor-m^2.

3.3.3. Air change efficiency

The air change efficiency (ACE) was between 60% and 70% with the PVRP depending on personalized airflow rate which was higher than with the DCV system (less than 50%). Therefore, the ventilation efficiency with the PVRP system was better than with the standard mixed ventilation (50%). As a result, a higher ACE can be created with the PVRP system and supplying less outdoor air, whereas the ACE of the DCV system is lower with larger airflow rate (118 - 153 l/s). This is because the nominal age of air of the PVRP system was longer than that of the DCV. Therefore, ACE was higher with the PVRP system according to Eq. (6) while the MAA was similar with both setups. Because the heat gain was distributed asymmetrically, the airflow was not fully mixed in the whole space. That led to 50 % of ACE with the DCV.

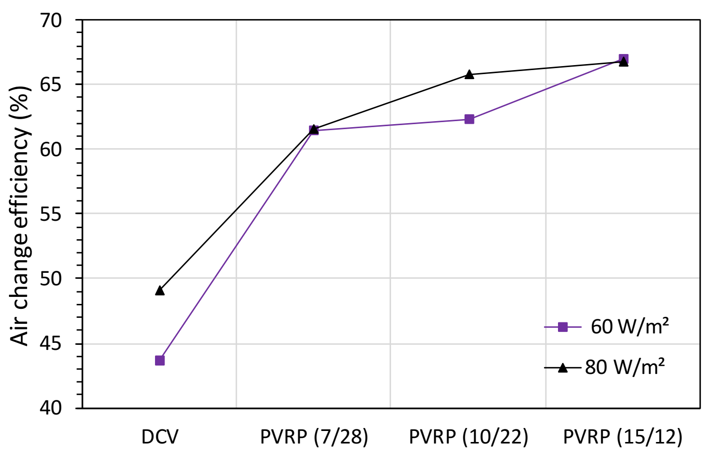

Fig. 7. ACE with the DCV and PVRP systems.

3.4. Thermal comfort

3.4.1. Temperature profile

The temperature at the reference location as well as the exhaust air temperature with the PVRP system were summarized in Table 6. Air temperature, operative temperature, mean radiant temperature and exhaust temperature all decreased with the increasing personalized airflow rate. With the PVRP system, increasing airflow rate from 7 l/s to 15 l/s decreased the temperature difference between the mean room air and operative temperature at 80 W/floor-m^2. The PVRP system created a significant temperature difference (from 0.2°C to 0.7°C) between the exhaust air and room air at the reference point, particularly with the higher personalized airflow rate. The higher heat gain made this difference more obvious. Therefore, better thermal comfort can also be achieved in the micro-environment near the workstation at the higher heat gain level. Average difference between the operative temperature and mean radiant temperature was rather small. This indicates that the radiant asymmetry was not a problem. The surface temperature of the simulated window was 33^{o}C and 39^{o}C with 60 W/m² and 80 W/m² and the wall surface temperature was 22^{o}C. Therefore, the maximum radiant temperature asymmetry due to the warm wall was 4^{o}C, which met Category A according to ISO 7730 standard [47]. This indicates the warm window did not cause thermal discomfort. The surface temperature of the heating foil and radiant panel were 34^{o}C and 20^{o}C, respectively. Therefore, the radiant temperature asymmetry due to the cool ceiling was 3.5^{o}C, which fulfilled the Category A also.

Fig. 8 shows the contribution of the convection flow to the mean temperature distribution at the horizontal level (1.1 m), from the corridor side and micro-environmen at the WS to the window side. Air temperature was increased gradually from the corridor to the window when the DCV system supplied the airflow evenly to the whole space. This was because the strenght of heat gain was decreased from the window to the corridor. The temperature of the DCV system were 0.8°C higher at the window side than the corridor side with 60 W/floor-m^2.

With the DCV as background ventilation (corridor side in Fig 1. a), the room air temperature of the PVRP was lowest close to the corridor side when the personalized flow rate was 7 l/s. The horizontal temperature differences of the PVRP system were between 0.4°C and 0.6°C. Thus, compared to the DCV, the horizontal temperature difference was smaller. With the higher personalized flow rate or less heat gain, the PVRP system can maintain a desirable temperature (below 26°C) in the micro-environment at WS.

Table 6

The average thermal conditions with the PVRP in different test cases.

Heat gain	Air flow rate of each PV terminal	Air temperature	Operative temperature	Mean radiant temperature	Exhaust air temperature	Average difference between operative and mean radiant temperature	Average difference between exhaust-room air temperature at the reference point
(W/m^2)	(l/s)	(°C)	(°C)	(°C)	(°C)	(°C)	(°C)
	7	26.3	26.4	26.4	26.5	-0.04	0.18
60	10	25.9	26.1	26.3	26.1	-0.17	0.24
	15	25.6	25.9	25.9	25.9	0.06	0.31
	7	26.6	26.3	26.4	26.7	-0.11	0.18
80	10	26.5	26.2	26.2	26.7	0.05	0.25
	15	25.9	25.9	26.0	26.5	-0.13	0.57

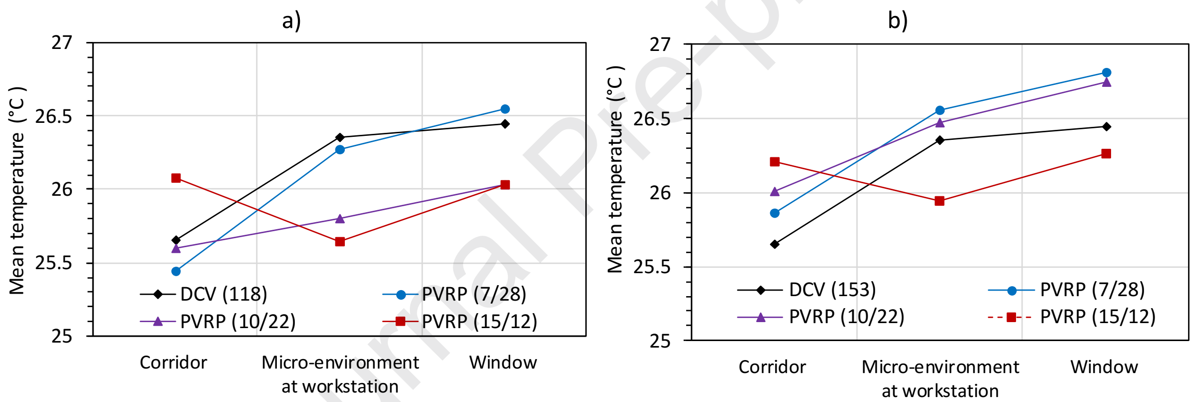

Fig. 8. The mean air temperature at 1.1 m with the DCV and PVRP systems at a) 60 W/floor-m^2 and b) 80 W/floor-m^2.

The mean room air temperatures near the dummy at vertical level with the PVRP (M1 – M3 in Fig.1a) and DCV (L9 and L10 in Fig.1b) systems were shown in Fig. 9. As shown in Fig. 9 a), the air temperature at 1.1 m height was 0.1-0.8°C lower with the PVRP than with the DCV at 60 W/floor-m^2. Only the highest personalized flow rate (15 l/s) was able to keep the air temperature near the dummy under 26°C at 80 W/floor-m^2 (Fig. 9b). The reason was the increased heat flux of the simulated window. Therefore, the strength and distribution of the heat gain have a notable effect on the vertical temperature distribution, which further affect the airflow pattern in the rooms.

The temperature distribution at the vertical level was quite different with the PVRP and DCV systems. However, in all the cases, the vertical differences were quite small. With the DCV, the room air temperature was highest near the dummy zone (more than 26°C) at 1.1 m height. Therefore, the all-air diffuse ceiling system cannot create the best thermal environment at the occupied zone in the studied room. With the PVRP, the lowest air temperatures were between the heights of 0.1 m to 1.1 m and the highest air temperatures occurred at 1.7 m level in most of the cases. When the PV airflow rate was increased, the vertical temperature profiles were quite similar, and the temperatures dropped down evenly at different heights. The vertical temperature difference in all the cases fulfilled the Category A of standard EN 15251 (2°C) [5].

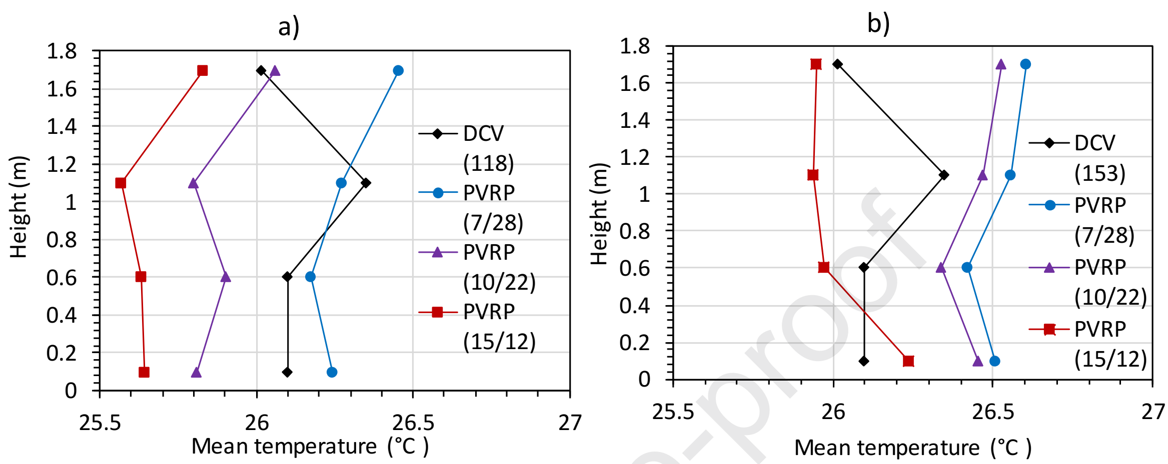

Fig. 9. The mean temperature difference at the vertical level with PVRP (M1 – M3) and DCV (L9 and L10) systems with a) 60 W/floor-m^2 and b) 80 W/floor-m^2.

3.4.2. Velocity profile

The horizontal distribution of the mean air velocity is shown in Fig. 10. The highest air velocity always occurred at the corridor side with the DCV. It happened because there was a large-scale circulating airflow pattern from the window side to the opposite corridor side created by the asymmetric heat load distribution. With the PVRP system (7 l/s), the trend of horizontal mean air velocity distribution was similar with the DCV system, but much lower (less than 0.1 m/s). The highest mean air velocity (above 0.12 m/s) at M1-M3 was measured micro-environment at the workstation with the PVRP when the personalized airflow rate was increased to 10 l/s and 15 l/s. The literature [50] proves that air velocity of a jet should be higher than 0.3 m/s to penetrate the breathing zone. In this study, air velocity close to the breathing zone was not measured. However, based on the smoke visualization (section 3.1), the airflow was strong enough to reach the breathing zone. Also, with the higher personalized flow rate, the air velocities at the window side and the corridor side decreased accordingly.

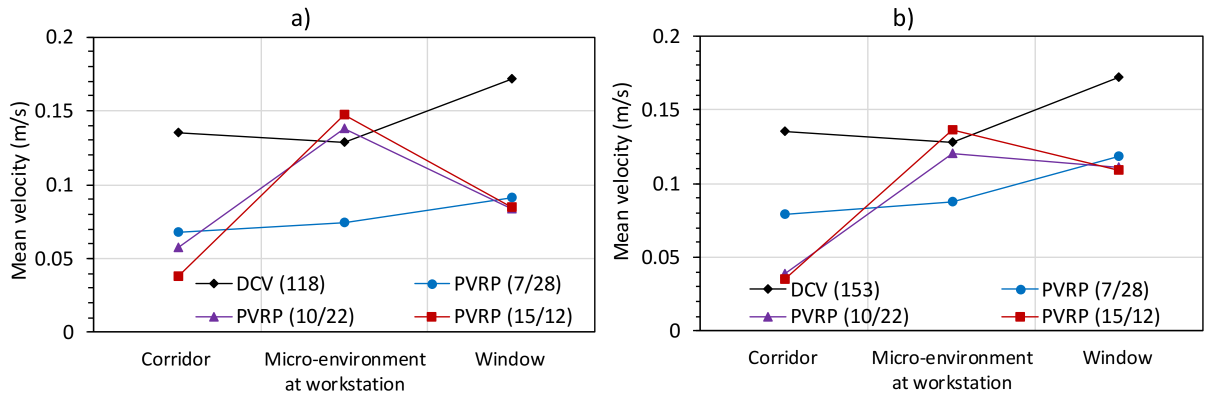

Fig. 10. The mean velocity distribution at the horizontal level with the DCV (L9 and L10) and PVRP (M1 – M3) systems at a) 60 W/floor-m^2 and b) 80 W/floor-m^2.

With the lowest personalized flow rate (7 l/s), the air velocity was low (less than 0.12 m/s) near the workstation at both heat gain levels in Fig. 11. The mean air velocities were able to fulfill the Category A [47] (0.12 m/s) demand with the PVRP (7 l/s). This indicates that the personalized airflow rate of 7 l/s did not cause unacceptable air movement at the measured locations nor significantly increase draught risk. When the supplied personalized airflow rate was 10 l/s or 15 l/s per person, the highest velocities were located between the heights of 1.1 m and 0.6 m at the two heat loads and met the category B requirement (0.18 m/s). The highest velocity occurred between the heights of 0.6 m and 1.1 m with the PVRP system because of the installation height of the PV ATD and gravity of cold air. However, it is clear that the highest velocity happened at 0.1 m height with the DCV system. Hence, the PVRP system had a potential to avoid thermal discomfort at the ankle level. When the personalized airflow rate was increased from 10 l/s to 15 l/s, the average velocity (P1-P3) between the heights of 0.1 and 1.1 m was increased from 0.09 m/s to 0.10 m/s with 60 W/floor-m^2 and 0.09 m/s to 0.12 m/s with 80 W/floor-m^2. The location in front of the dummy was not measured. The air movement may cause discomfort for sensitive occupants, but in a real application, the personal control can avoid this risk.

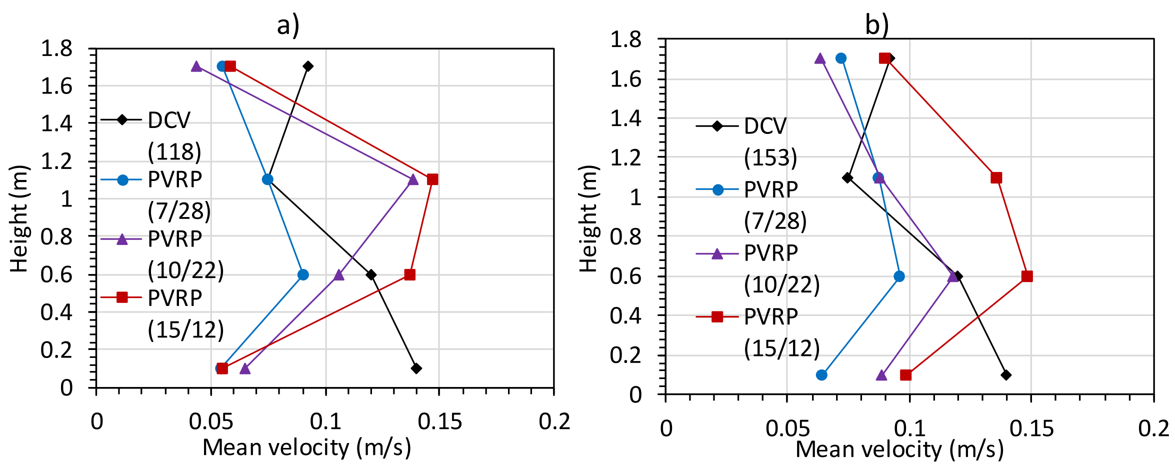

Fig. 11. The mean air velocity distribution at the vertical level under the PVRP (M1 – M3) and DCV (L9 and L10) systems with a) 60 W/floor-m^2 and b) 80 W/floor-m^2.

3.4.3. Local thermal discomfort

With the both systems, the draught risk (DR) was relatively low in all the cases (Fig. 12), The highest DR happened at the heights of 0.6 – 1.1 m with the PVRP system which was similar with the air velocity distribution. With the lower personalized airflow rate, DR was below 10% with the PVRP system. When the personalized flow rate was increased to 15 l/s, the draught risk increased to 12 % and 18 % at the 1.1 m height level at 60 W/floor-m^2 and 80 W/floor-m^2, respectively. Hence, heat gain also had an obvious effect on the draught rate with the PVRP system. With the DCV system, the draught risk at the 1.1 m height was also low (6 %). However, the draught risk at the ankle level (0.1 m) was much higher with the DCV (10 %) than with the PVRP (less than 5%). The reason for the high draught risk of the DCV at the floor level was the return flow created from the corridor by the convection flows.

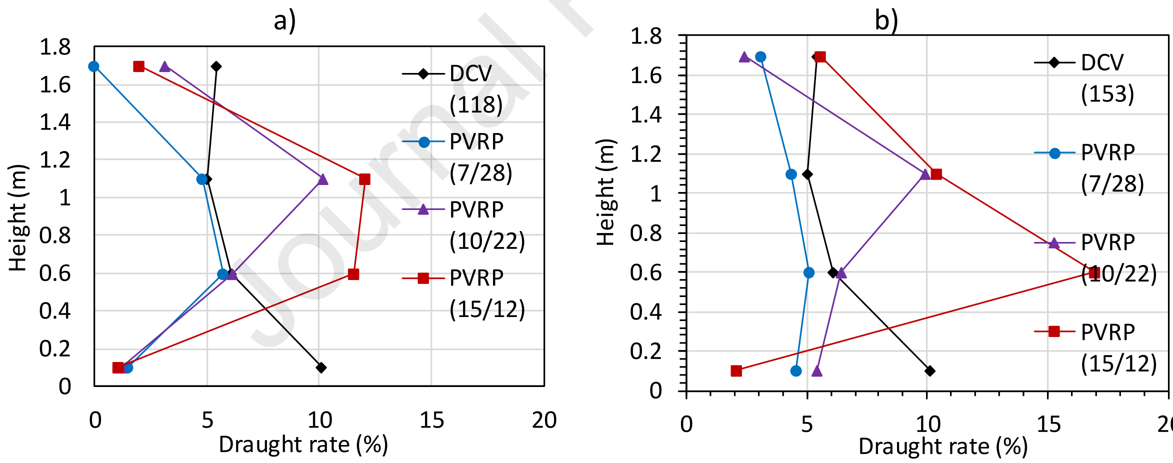

Fig. 12. Draught risk under the PVRP (M1 – M3) and DCV (L9 and L10) systems with a) 60 W/floor-m^2 and b) 80 W/floor-m^2.

4. Discussion

The PVRP system enables the creation of a micro-environment where the local indoor climate can be individually controlled by each user. Therefore, it makes the simultaneous reduction of energy consumption and enhancement of indoor air quality and thermal comfort. From the energy saving perspective, the demand-controlled local environment has a remarkable potential in modern commercial buildings where people spend just part of the day at their own workstations.

The elaborating air velocity can enhance the thermal sensation in a hot environment. Thus, the air velocity is one factor to improve the thermal comfort in an energy efficient manner. However, if the air velocity is too high, the thermal discomfort will occur. With the PVRP system, the airflow was supplied directly to the dummy, but the local draught risk was not found to significantly increase. However, draught risk would be higher near the face. In real applications users can control their personalized airflow rates and direction and thus the actual risk of draught is even lower.

It is well-known that the metabolic rates estimated from the measurements of CO_2 agree well with the range of metabolic rates recorded in large field studies in offices [51]. Based on CO_2 concentration and the known ventilation rate, it has been indicated that metabolic rates decreased when the ventilation rate decreased [52]. One logical explanation is that increased muscle tonus at higher work rates explains the higher metabolic rate at increased ventilation rate [53]. Another underlying mechanism could be that subjects may unconsciously reduce their breathing rate at low ventilation rates. This indicates that metabolic rate is not constant during working hours and it varies depending on activity level. Also unconsciously reduced breathing rate could be a significant factor and this supplementary hypothesis requires more validations in future studies.

The vertical temperature (<0.3°C) near the workstation was negligible with the PVRP compared to the Category A (3°C) of ISO 7730 standard [47]. The temperature difference between the workstation and exhaust was maximum 0.6°C. This indicates the energy saving potential by using the PVRP system. For the practical usage, the higher local airflow rate increases the air movement and enhance thermal sensation for a human subject. In the study, we focused on physical measurements without human subject test.

From the aspect of ventilation efficiency, the PVRP system achieved higher air change efficiency (ACE) compared to fully mixed ventilation. The reason was that the airflow structure of the PV diffuser can be considered as displacement type flow which performs between fully mixed flow (50%) and ideal piston flow (100%). Hence, the performance regarding the ventilation efficiency of the PVRP system was similar with that of the displacement ventilation. As for the local air change index (LAC), the values measured at the dummy was much higher than 100%. Thus, air change index with the PVRP was better than the mixed ventilation (100%). Compared to the traditional method where the fresh air is supplied far from the occupants, the PV ATD installed in front of the occupant supplies the clean air more straightly to the occupants. Therefore, less contaminants are induced within the clean supply air before it arrives the breathing zone, possibly improving the perception of air quality.

It has been proven that PV combined with the mixing ventilation or displacement ventilation provides a better indoor environment compared to the use of traditional mechanical ventilation alone [27]. Also, desk fans near the occupants can be used to improve thermal comfort by increasing air movement. Still, it has been noted that as a result of increasing air movement, some people feel draught and to solve this problem, radiant cooling has been introduced.

The PVRP system combined with the diffuse ceiling ventilation introduced in this study can simultaneously provide good indoor air quality and low draught risk. The localized radiant cooling can decrease the convective flow around a human body and improve the perceived air quality (PAQ) acceptability. However, this improvement is not as obvious as what can be provided with the convective cooling by rising the air movement [54].

The complicated thermal experiences of occupants have notable effect on their thermal comfort e.g. their behaviour, physiology and psychology conditions [55]. Therefore, there should be an individually controlled environment to meet the variable responses whenever necessary. The PVRP system makes it possible to control the airflow rate (local velocity) of the personalized air to customize the environment according to the individual preferences. It should be noted that some users may choose low personalized airflow rate and supply air at high temperatures in order to feel comfortable. Therefore, the background ventilation should be adapted in conjunction with the PV in the space especially when the high heat and/or pollution loads exist.

The analyzed system is to some extent restricted by the set-up of the space, affecting the possible radiant panel installation both from height and size perspectives. In order to maximize efficiency, the application of this system needs careful consideration of the type and location of the personal ventilation ATD and WS in relation to the geometry of the ventilated space. A properly designed PVRP system would lead to substantially lower temperature in the micro-environment and thus further improve the perceived air quality (PAQ) acceptability compared to the traditional mechanical ventilation.

According to the physical measurement, the air quality and thermal comfort were improved at the target micro-environment. The application of the PVRP system in other building types should be further studied. The human subject test should be carried out to study thermal sensation with different airflow rates and flow directions with individual control. The highest accepted air velocity could be used as starting point to further study the effect of air movement on temperature difference between the occupied zone and exhaust. The performance of the PVRP system with different varied metabolic rates should be further studied and analyzed the possible effects of metabolic rate on the indoor thermal environment. Based on of these, it is possible to estimate potential energy saving more accurately.

5. Conclusion

The objective of this paper was to compare the performance of the personalized ventilation combined with the radiant panel system (PVRP) to that of the diffuse ceiling all-air ventilation system (DCV) experimentally. The airflow pattern, indoor air quality and thermal comfort were analyzed in the test chamber.

The smoke visualization showed that the personalized ventilation air terminal devices supplied the fresh air horizontally to the occupants and created a micro-environment around the dummy.

Heat removal efficiency was higher with the PVRP system combined with the perimeter exhaust than with the DCV system alone even with much lower airflow rate.

The results show that MAA was shorter with the PVRP (22.6 minutes) than that with the DCV (25.2 minutes) near the dummy. Increasing personalized airflow rate decreased MAA near the dummy. Also, the ACE was higher than 60% by using the PVRP system and increased with the personalized airflow rate while it was around 50% when using the DCV.

The mean temperature in the micro-environment at the workstation when using the PVRP system was below 26°C with the higher personalized airflow rate or lower heat gain, which is 0.1-0.8°C lower than with the DCV system. With the PVRP system combined with the perimeter exhaust, the temperature in the micro-environment was 0.2°C-0.7°C lower than the exhaust temperature. Spot cooling was achieved at the workstation with these devices. With the higher personalized airflow rate, the velocity at 0.1 m height can remain at a reasonable value without draught risk.

Declaration of competing interest

The authors declare that they have no known competing financial interests or personal relationships that could have appeared to influence the work reported in this paper.

Acknowledgement

The author wishes to acknowledge the funder of Aalto scholarship. The author wishes to acknowledge the personal ventilation units provided by Prof. Arsen K Melikov from Technical University of Denmark.

References

[1] O. Seppänen, Scientific basis for design of ventilation for health , productivity and good energy efficiency, Indoor Air Congr. (2008) 17–22.

[2] O. Seppänen, Ventilation strategies for good indoor air quality and energy efficiency, in: Int. J. Vent., 2008: pp. 297–306. https://doi.org/10.1080/14733315.2008.11683785.

[3] B. Yang, S.C. Sekhar, The influence of evenly distributed ceiling mounted personalized ventilation devices on the indoor environment, Int. J. Vent. 7 (2008) 99–112. https://doi.org/10.1080/14733315.2008.11683803.

[4] P. Wargocki, D.P. Wyon, Ten questions concerning thermal and indoor air quality effects on the performance of office work and schoolwork, Build. Environ. 112 (2017) 359–366. https://doi.org/10.1016/j.buildenv.2016.11.020.

[5] CEN 15251. Indoor environmental input parameters for design and assessment of energy performance of buildings addressing indoor air quality, thermal environment, lighting and acoustics. European Committee for Standardization, Brussels, Belgium, 2007

[6] Danish Standard, DS/CEN/CR 1752. Ventilation for buildings – Design criteria for the indoor environment., Int. Organ. Stand. (2001) 2920.

[7] R.L. Hedrick, W.R. Thomann, H. Aguilar, L.A. Damiano, A.K.H. Darwich, G. Gress, H. Habibi, E.P. Howard, L.G. Petrillo-groh, J.K. Smith, S.D. Williams, P.L. Doppel, H.D. Davis, F.J. Fisher, W.E. Morris, J.W.W. Olsen, R.L. Hall, D.T. Reindl, J.R. Anderson, C.S. Barnaby, J.A. Clark, P.T. Graef, Ventilation for acceptable indoor air quality: ANSI/ASHRAE Standard 62.1-2013, ASHRAE Stand. (2015).

[8] P. Ole Fanger, Indoor air quality in the 21st century: Search for excellence, Indoor Air. 10 (2000) 68–73. https://doi.org/10.1034/j.1600-0668.2000.010002068.x.

[9] S. Lestinen, S. Kilpeläinen, R. Kosonen, J. Jokisalo, H. Koskela, Experimental study on airflow characteristics with asymmetrical heat load distribution and low-momentum diffuse ceiling ventilation, Build. Environ. 134 (2018) 168–180. https://doi.org/10.1016/j.buildenv.2018.02.029.

[10] W. Wu, N. Yoon, Z. Tong, Y. Chen, Y. Lv, T. Ærenlund, J. Benner, Diffuse ceiling ventilation for buildings: A review of fundamental theories and research methodologies, J. Clean. Prod. 211 (2019) 1600–1619. https://doi.org/10.1016/j.jclepro.2018.11.148.

[11] P. V Nielsen, The “Family Tree” of Air Distribution Systems, in: Roomvent 2011, 2001.

[12] P. Heiselberg, S. Murakami, R. Claude-Alain, Ventilation of large spaces in buildings, Analysis and Prediction Techniques, Energy Conserv. Build. Community Syst. Annex 26 Energy Effic. Vent. Large Enclosures. (1998).

[13] A.K. Melikov, Advanced air distribution: Improving health and comfort while reducing energy use, Indoor Air. 26 (2016) 112–124. https://doi.org/10.1111/ina.12206.

[14] M. Fountain, F. Bauman, E. Arens, K. Miura, R. de Dear, Locally controlled air movement preferred in warm isothermal environments, in: ASHRAE Trans., 1994: pp. 937–952.

[15] Y. Zhai, H. Zhang, Y. Zhang, W. Pasut, E. Arens, Q. Meng, Comfort under personally controlled air movement in warm and humid environments, Build. Environ. 65 (2013) 109–117. https://doi.org/10.1016/j.buildenv.2013.03.022.

[16] S. Goyal, H.A. Ingley, P. Barooah, Occupancy-based zone-climate control for energy-efficient buildings: Complexity vs. performance, Appl. Energy. 106 (2013) 209–221. https://doi.org/10.1016/j.apenergy.2013.01.039.

[17] S. Purdon, B. Kusy, R. Jurdak, G. Challen, Model-free HVAC control using occupant feedback, in: Proc. - Conf. Local Comput. Networks, LCN, 2013: pp. 84–92. https://doi.org/10.1109/LCNW.2013.6758502.

[18] F. Oldewurtel, D. Sturzenegger, M. Morari, Importance of occupancy information for building climate control, Appl. Energy. 101 (2013) 521–532. https://doi.org/10.1016/j.apenergy.2012.06.014.

[19] Y. He, X. Wang, N. Li, M. He, D. He, Heating chair assisted by leg-warmer: A potential way to achieve better thermal comfort and greater energy conservation in winter, Energy Build. 158 (2018) 1106–1116. https://doi.org/10.1016/j.enbuild.2017.11.006.

[20] S. Shahzad, J.K. Calautit, K. Calautit, B. Hughes, A.I. Aquino, Advanced personal comfort system (APCS) for the workplace: A review and case study, Energy Build. 173 (2018) 689–709. https://doi.org/10.1016/j.enbuild.2018.02.008.

[21] S. Watanabe, A.K. Melikov, G.L. Knudsen, Design of an individually controlled system for an optimal thermal microenvironment, Build. Environ. 45 (2010) 549–558. https://doi.org/10.1016/j.buildenv.2009.07.009.

[22] X. Shao, X. Li, X. Ma, C. Liang, Multi-mode ventilation: An efficient ventilation strategy for changeable scenarios and energy saving, Build. Environ. 115 (2017) 332–344. https://doi.org/10.1016/j.buildenv.2017.01.032.

[23] S. Zhang, Y. Lu, Z. Lin, Coupled thermal comfort control of thermal condition profile of air distribution and thermal preferences, Build. Environ. 177 (2020). https://doi.org/10.1016/j.buildenv.2020.106867.

[24] M. Luo, E. Arens, H. Zhang, A. Ghahramani, Z. Wang, Thermal comfort evaluated for combinations of energy-efficient personal heating and cooling devices, Build. Environ. 143 (2018) 206–216. https://doi.org/10.1016/j.buildenv.2018.07.008.

[25] A.K. Melikov, Personalized ventilation, Indoor Air, Suppl. 14 (2004) 157–167. https://doi.org/10.1111/j.1600-0668.2004.00284.x.

[26] A.K. Melikov, Improving Comfort and Health By Personalized Ventilation, Ashrae Stand. (2004) 1–12.

[27] R. Cermak, A.K. Melikov, L. Forejt, O. Kovar, Performance of personalized ventilation in conjunction with mixing and displacement ventilation, HVAC R Res. 12 (2006) 295–311. https://doi.org/10.1080/10789669.2006.10391180.

[28] R. Li, S.C. Sekhar, A.K. Melikov, Thermal comfort and IAQ assessment of under-floor air distribution system integrated with personalized ventilation in hot and humid climate, Build. Environ. 45 (2010) 1906–1913. https://doi.org/10.1016/j.buildenv.2010.03.003.

[29] M. Dalewski, A.K. Melikov, M. Vesely, Performance of ductless personalized ventilation in conjunction with displacement ventilation: Physical environment and human response, Build. Environ. 81 (2014) 354–364. https://doi.org/10.1016/j.buildenv.2014.07.011.

[30] M. Taheri, M. Schuss, A. Fail, A. Mahdavi, A performance assessment of an office space with displacement, personal, and natural ventilation systems, Build. Simul. 9 (2016) 89–100.

https://doi.org/10.1007/s12273-015-0252-5.

[31] T. Arghand, T. Karimipanah, H.B. Awbi, M. Cehlin, U. Larsson, E. Linden, An experimental investigation of the flow and comfort parameters forunder-floor, confluent jets and mixing ventilation systems in an open-plan office, Build. Environ. 92 (2015) 48–60. https://doi.org/10.1016/j.buildenv.2015.04.019.

[32] F. Alamdari, D.J.G. Butler, P.F. Grigg, M.R. Shaw, Chilled ceilings and displacement ventilation, Renew. Energy. 15 (1998) 300–305. https://doi.org/10.1016/s0960-1481(98)00177-3.

[33] K.N. Rhee, K.W. Kim, A 50 year review of basic and applied research in radiant heating and cooling systems for the built environment, Build. Environ. 91 (2015) 166–190. https://doi.org/10.1016/j.buildenv.2015.03.040.

[34] G. Sastry, P. Rumsey, VAV vs. radiant: Side-by-side comparison, ASHRAE J. (2014).

[35] W. Zhao, S. Kilpeläinen, R. Kosonen, J. Jokisalo, Experimental comparison of local low velocity unit combined with radiant panel and diffuse ceiling ventilation systems, Indoor Built Environ. 29 (2020) 895–914. https://doi.org/10.1177/1420326X20918398.

[36] W. Zhao, S. Lestinen, S. Kilpeläinen, R. Kosonen, Comparison of the effects of symmetric and asymmetric heat load on indoor air quality and local thermal discomfort with diffuse ceiling ventilation. Accepted for publication in the International Journal of Ventilation 22 July 2019.

[37] D. Zukowska, A. Melikov, Z. Popiolek, Impact of geometry of a sedentary occupant simulator on the generated thermal plume: Experimental investigation, in: HVAC R Res., 2012: pp. 795–811. https://doi.org/10.1080/10789669.2012.672925.

[38] A. Mishra, M. Loomans, R. Kosonen, Actimetry for estimating occupant activity levels in buildings: A step toward optimal and energy-efficient indoor conditioning, IEEE Consum. Electron. Mag. 8 (2019) 67–71. https://doi.org/10.1109/MCE.2018.2867983.

[39] Y. Zhai, M. Li, S. Gao, L. Yang, H. Zhang, E. Arens, Y. Gao, Indirect calorimetry on the metabolic rate of sitting, standing and walking office activities, Build. Environ. (2018). https://doi.org/10.1016/j.buildenv.2018.09.011.

[40] T. Palomar, M. Silva, M. Vilarigues, I. Pombo Cardoso, D. Giovannacci, Impact of solar radiation and environmental temperature on Art Nouveau glass windows, Herit. Sci. 7 (2019). https://doi.org/10.1186/s40494-019-0325-3.

[41] J. Sengupta, K.S. Chapman, A. Keshavarz, Window performance for human thermal comfort, in: ASHRAE Trans., 2005: pp. 254–275.

[42] CEN (European Committee for Standardization), Ventilation for non-residential buildings - Performance requirements for ventilation and room conditioning systems, Ital. Stand. (2005) 1–75.

[43] E. Sugawara, H. Nikaido, Properties of AdeABC and AdeIJK efflux systems of Acinetobacter baumannii compared with those of the AcrAB-TolC system of Escherichia coli, Antimicrob. Agents Chemother. 58 (2014) 7250–7257. https://doi.org/10.1128/AAC.03728-14.

[44] M. Embaye, R.K. Al-Dadah, S. Mahmoud, Numerical evaluation of indoor thermal comfort and energy saving by operating the heating panel radiator at different flow strategies, Energy Build. 121 (2016) 298–308. https://doi.org/10.1016/j.enbuild.2015.12.042.

[45] P. V Nielsen, F. Allard, H.B. Awbi, L. Davidson, A. Schälin, Computational Fluid Dynamics in Ventilation Design REHVA Guidebook No 10, Int. J. Vent. 6 (2007) 291–294. https://doi.org/10.1080/14733315.2007.11683784.

[46] A.K. Melikov, Z. Popiolek, M.C. Silva, I. Care, T. Sefker, Accuracy limitations for Low-

Velocity measurements and draft assessment in rooms, HVAC R Res. 13 (2007) 971–986. https://doi.org/10.1080/10789669.2007.10391465.

[47] ISO, ISO 7730: Ergonomics of the thermal environment Analytical determination and interpretation of thermal comfort using calculation of the PMV and PPD indices and local thermal comfort criteria, Management. (2005).

[48] S. Zhang, Y. Cheng, C. Huan, Z. Lin, Heat removal efficiency based multi-node model for both stratum ventilation and displacement ventilation, Build. Environ. 143 (2018) 24–35. https://doi.org/10.1016/j.buildenv.2018.06.054.

[49] M. Sandberg, What is ventilation efficiency?, Build. Environ. 16 (1981) 123–135. https://doi.org/10.1016/0360-1323(81)90028-7.

[50] D. Licina, A. Melikov, C. Sekhar, K.W. Tham, Human convective boundary layer and its interaction with room ventilation flow, Indoor Air. 25 (2015) 21–35. https://doi.org/10.1111/ina.12120.

[51] R.J. de Dear, M.E. Fountain, Field experiments on occupant comfort and office thermal environments in a hot-humid climate, in: ASHRAE Trans., 1994: pp. 457–474.

[52] P. Wargocki, The effects of outdoor air supply rate in an office on perceived air quality, sick building syndrome (SBS) symptoms and productivity, Indoor Air. (2000). https://doi.org/10.1034/j.1600-0668.2000.010004222.x.

[53] D.P. Wyon, P.O. Fanger, B.W. Olesen, C.J. Pedersen, The mental performance of subjects clothed for comfort at two different air temperatures, Ergonomics. (1975). https://doi.org/10.1080/00140137508931470.

[54] A.K. Melikov, B. Krejciríková, J. Kaczmarczyk, M. Duszyk, T. Sakoi, Human response to local convective and radiant cooling in a warm environment, HVAC R Res. 19 (2013) 1023–1032. https://doi.org/10.1080/10789669.2013.842734.

[55] H. Liu, Y. Wu, B. Li, Y. Cheng, R. Yao, Seasonal variation of thermal sensations in residential buildings in the Hot Summer and Cold Winter zone of China, Energy Build. 140 (2017) 9–18. https://doi.org/10.1016/j.enbuild.2017.01.066.

Highlights

- comparison of personal ventilation with radiant panel (PVRP) and all-air system
- the perimeter exhaust over window increases heat removal efficiency
- the air change efficiency with PVRP is over 60%, much higher than fully mixed flow
- the temperature difference between occupied and exhaust could be 0.6^{c}C with PVRP
- the draught risk remains at acceptable level at occupied zone with PVRP

Declaration of competing interest

The authors declare that they have no known competing financial interests or personal relationships that could have appeared to influence the work reported in this paper.